SciEn
Proceedings of 8th International Conference on Mechanical Engineering and Renewable Energy 2025
10-12 December, 2025, Chattogram, BANGLADESH
SciEn Conference Series: Engineering Vol. 4, 2026, pp 195-200 https://doi.org/10.38032/scse.2026.4.103

Autonomous Threat Assessment and Maneuver Control for Unarmed Ships Using ML-Based Pirate Detection

Md. Sabbir Ahmed, Zobair Ibn Awal*

Department of Naval Architecture and Marine Engineering, Bangladesh University of Engineering and Technology, Dhaka 1000, Bangladesh.

ABSTRACT

This study proposes an end-to-end, machine-learning-driven maritime security system that combines a YOLOv8-based object-detection pipeline trained on an augmented dataset encompassing low-light and adverse-weather conditions with a probabilistic threat-level assessment module. By incorporating vessel characteristics such as size, speed, and heading, our framework distinguishes between potential pirate skiffs and benign craft (e.g., refugee boats), thereby minimizing false positives. Upon detecting a hostile vessel, the system estimates its range and velocity relative to the merchant ship and computes an optimal evasive response. In particular, the results demonstrates that zigzag maneuvering consistently yields the highest probability of repelling an attack when the vessel is unarmed. Our approach is designed for real-time operation on commodity computing hardware and provides a proof-of-concept pathway toward early threat mitigation at sea.

Keywords: YOLOv8, Threat Detection, Nomoto Model, Vessel Control, Maritime Security.

1. Introduction

Maritime transport is the backbone of global economic integration, providing cost-effective and reliable connectivity between producers and consumers across continents. Over 23 million tonnes of cargo daily and about 55,000 passengers traverse international sea routes, highlighting shipping's unmatched capacity for bulk movement and its essential role in modern supply chains [1]. On an annual scale, the sector moves roughly 6 billion tonnes of merchandise, equivalent to about 80 % of global trade by volume, through a fleet of over 93,000 merchant vessels, supported by a workforce of 1.25 million [2].

However, adopting automated navigation, engine, and communication systems has reduced crew sizes, limiting visual lookout capacity. Semi-submerged skiffs and AIS-less "dark" vessels can evade detection, especially at night or in poor visibility, exploiting gaps in radar coverage and vast patrol areas. This diminished vigilance, coupled with a reliance on AIS and post-detection mitigation [3], has contributed to renewed piracy in high-risk regions, where slower, lightly defended merchant vessels are prime targets. Table 1 lists the most affected chokepoints from 2019 to 2024.

One of the most significant recent incidents was the March 2024 hijacking of the Bangladeshi-flagged MV *Abdullah* by Somali pirates, approximately 600 nautical miles east of Mogadishu, within the Indian Ocean piracy zone. The ship and its crew were released only after a ransom of $5 million was paid [4], highlighting both the financial and human risks associated with maritime piracy, as illustrated in Tables 2 and 3.

Table 1 Region-Based Piracy Attack (2019-2024), [5]

Sea Lane	Pirate Attacks Over the Year					
	2019	2020	2021	2022	2023	2024
Malacca, Singapore Straits	45	48	69	72	85	91
West Africa	67	90	38	21	22	17
South China Sea	34	37	16	4	14	10
Indian Ocean	10	12	5	9	5	19
Others	41	42	44	25	24	9

Table 2 Impact on Crew (Author's calculation, [5])

Year	2020	2021	2022	2023	2024	Total	Attack on crew/Year
Lives lost	0	3	0	2	0	5	
Wounded crew	10	5	1	4	3	23	
Missing crew	28	1	0	0	0	29	486/5 =97.2
Crew hostage	107	48	24	92	132	403	
Assaulted	8	1	6	2	9	26	

*Corresponding Author Email Address: sabbir.name.buet@gmail.com

Table 3 Total Estimated Cost due to piracy (2010-2021) [6], [7]

Time frame & region	Cost estimate (USD)
2010 – Somali piracy	$7 – 12 billion
2011 – Somali piracy	$6.6 – 6.9 billion
2012 – Somali piracy	$5.7 – 6.1 billion
2013 – Somali piracy	$3 billion
2014 – Western Indian Ocean	$2.3 billion
2015 – West Africa	$719.6 million
2016 – West Africa	$793.7 million
2017 – West Africa	$809.6 million
2018 – West Africa	$820 million
2019 – West Africa	$1.925 billion
2020 – West Africa	$1.9 billion
2021 – West Africa	$1.94 billion

Somali piracy peaked in 2010 but was brought under control through enhanced naval patrols and Best Management Practices (BMP), leading to a steady decline in costs by 2013 (Table 3). From 2014 onward, attacks shifted to the Western Indian Ocean and West Africa (Gulf of Guinea), where kidnappings for ransom, reflected in the surge of crew hostages (Table 2), became the dominant tactic. Consequently, annual piracy costs in these regions rose from $719.6 million in 2015 to $1.94 billion in 2021, more than doubling over that period (Table 3).

2. Present Piracy Prevention System

The rise of organized piracy has compelled the maritime sector to bolster its defenses against unforeseen threats. This defense system can be categorized into a. detection and b prevention (pre-boarding and post-boarding measures) [8].

Current anti-piracy measures employ a range of surveillance and interdiction technologies. Satellite-based systems such as Synthetic Aperture Radar (SAR) and Automatic Identification System (AIS) networks enable broad-area vessel monitoring, while UAVs with machine-learning analytics support rapid anomaly detection and classification [9]. Classifiers including CNNs, Decision Trees, Naive Bayes, and Random Forests have been applied to ship detection, with recent YOLO-based models achieving high accuracy for conventional vessels [10]. However, due to constrained dataset diversity, these approaches often falter when confronted with small craft (e.g., pirate skiffs) and lack the contextual understanding necessary to infer vessel intent.

Non-lethal countermeasures, including water cannons, acoustic hailing devices, and prescribed evasive maneuvering techniques, further deter hostile approaches [9]. Indeed, Shane et al. (2015) conducted a large-scale analysis of 452 pirate attack incidents worldwide, coding the use of various defensive measures lookouts, alarms, security guards and zigzagging and employing regression models to evaluate their efficacy; they found that "evasive maneuvers" conferred the most significant protective effect, with an odds ratio of approximately 27, far surpassing all other tactics examined [11].

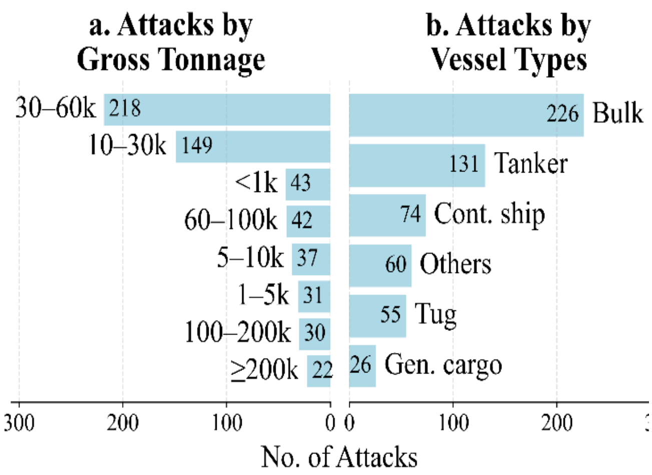

Fig. 1 Distribution of piracy attacks by GT; (b) Distribution of piracy attacks by vessel type, between the years 2021-2024 (Author's calculation, [5])

Because of size constraints and complexity, many vessels cannot be fitted with comprehensive anti-piracy systems. Moreover, in recent years, pirates have shifted their focus from large commercial ships to smaller and medium-sized vessels operating close to shore, which are less well-protected and easier to board [7]. Indeed, between 2021 and 2024, vessels of 10,000–29,999 GT endured approximately 149 attacks, and those of 30,000–59,999 GT suffered about 218, whereas ships over 100,000 GT faced only around 52 incidents (IMO), illustrated in Fig. 1. And according to the type of vessel bulk carrier (225 times) was more frequently attacked, followed by the tanker (140 times) and the container vessel (75 times).

2.1 Research Gap

Existing systems lack continuous monitoring, preventing real-time capable detection and tracking of illicit activity at sea [8]. This study presents an integrated detection–prevention framework for unarmed vessels, combining real-time image analysis with optimal evasive maneuvers to enhance crew safety across diverse vessel types and threat ranges, while reducing reliance on costly piracy-prevention systems.

3. Automated Anti-Piracy Framework

This data for detecting piracy objects was selected after studying several piracy incidents. The most used vessel type by the pirates is a canoe, fishing boat, skiff, speedboat, and the most used weapons are crowbar, gun, knife, machete, and rifle. The weapon and vessel types may vary, but for the initial experiment, this data was taken based on 1691 documented piracy incidents out of 1975 recorded incidents between 2015 and 2024 [5]. The life raft boat is also included with the vessel types to differentiate between the pirates and potential refugees. The zigzag [11] mode was compared with the straight heading evasion for the unarmed situation.

The end-to-end (video-to-decision) pipeline integrates machine learning based object detection with automated threat assessment and decision making, as illustrated in Fig. 2.

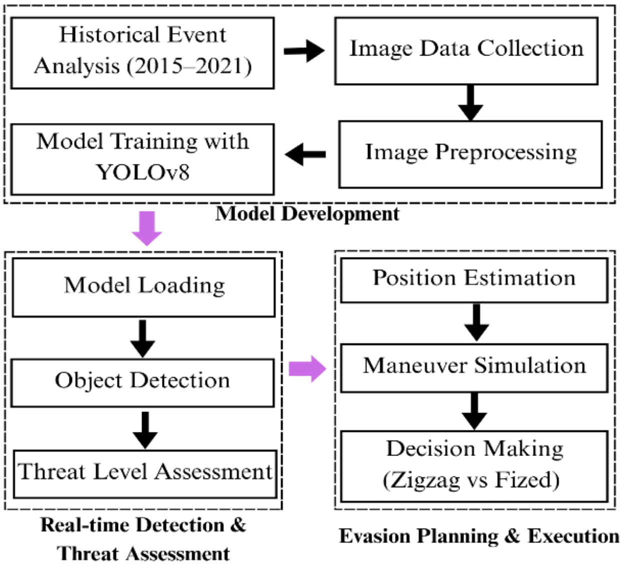

Fig. 2 Automated Piracy-Detection

3.1 Model Development

a. Data Collection

A custom dataset from open-source piracy incident images was labeled manually in Roboflow (private workspace) [12]. Dataset access is restricted to maintain compliance with original image copyrights. Labeling the dataset was done manually.

a. b. c. d.

Fig. 3 Data Augmentation (a. original, b. blurred with water droplet effect, c. night vision, and d. IR)

b. Image Preprocessing

To enhance robustness, 25% of the dataset was augmented (Fig. 3). The final training set comprised 13,449 images for vessel types and 21,887 for weapons (Table 4).

Table 4 Dataset split for training, testing, and validation

Model	**Train Images**	**Test Images**	**Validation Images**	**Percentage Split**
Pirate Vessel Detection	12,776	852	3408	Train (75%)/ Test (5%) / Val (20%)
Weapon Detection	21,180	1,385	4,156	Train (80%)/ Test (5%) / Val (15%)

The YOLOv8 model was trained on Kaggle's T4 GPUs for efficient computation. Table 5 summarizes the key hyperparameters.

Table 5 Hyperparameters used in the model

Category	**Hyperparameter**	**Value**
Training	Epochs	100
	Batch size	16
	Image size (px)	640 × 640
Optimization	Optimizer	AdamW
	LR	1.0×10^{-4}
	β1	0.9
	WD	0.0005
Augmentation	Mosaic	✓
	MixUp	✓
Validation	Enabled	✓

3.2 Threat Assessment

A raw threat score is computed based on vessel type, weapons detected, crew count, range to target, and pirate vessel speed. Range d [m] is estimated using the pinhole-geometry model in Eq. (1)

$$d = \frac{f.h.C}{y - y_{horizon}} \quad (1)$$

Where, f[px] is focal length, h [m] mounting height above sea level, C is a calibration constant, y [px] vessel base coordinate, and $y\_horizon$ [px] horizon coordinate. Relative speed v [m/s] is computed from Eq. (2)

$$v = \frac{\Delta x.d}{f.\Delta t} \quad (2)$$

where Δt [s] is the interframe time interval. Continuous d and v estimates are compared against thresholds to trigger the Nomoto-based evasive maneuver logic.

3.3 Evasive Maneuvering

A first-order Nomoto model [13] links the commanded rudder angle to the vessel's yaw rate via a single time constant and gain:

$$T\dot{r} + r = K\delta \quad (3)$$

Eq. (3), $d\psi/dt = r$ [rad/s], ψ [rad] is heading, r is the yaw rate, δ [rad] is the rudder angle, T[s] and K[1/s] are the Nomoto indices (time constant and gain).

a. Parameters

Parameters reflect the moderately maneuverable bulk carrier *MV Abdullah* (attacked 12 March 2024), listed in Table 6. Rudder area A_R 42 m^2[14] and K' and T' for the first-order Nomoto model are from [15].

Table 6 MV Abdullah Parameters [16]

Parameter	**Bulk carrier**
Length overall, L_M (m)	189
Breadth, B_M (m)	32
Draft, T_M (m)	12.95
Block coefficient, C_β	0.8
Rudder area, A_r (m^2)	42
Nondimensional Time Constant, T'	5.1
Nondimensional gain, K'	3.85

Pirate vessel parameters are based on small fast craft (canoes, fishing boats, skiffs, speedboats) ranging from 6–20 m long. Beam and draft are estimated as $B_P = L_P/3.5$ and $D_P = L_P/7$ [17], with a uniform speed of 25 knots. The speed is taken as 25 knots for all sizes of pirate vessels. Attacker guidance follows a line-of-sight or pure pursuit strategy. Vessel size is derived using the pinhole principle, where each object points projects through the camera aperture to the image plane. $L_p = bb_w \times bb_d/f_C$. Here, L_P, B_P, D_P is respectively the length, breadth and depth of the pirate vessel, bb_w maximum bounding-box width [px], bb_d is range [m], f_c is camera's focal length [px]. Using these particulars, capsizing significant wave height and period are estimated as $H_{crt} = 0.37L,\ T_{crt} = 0.39L$ [17].

b. Speed Loss

The merchant vessel's rudder angle and speed were adjusted to match the desired wave height and frequency. Since larger rudder angles cause greater speed loss, a 10° rudder angle was selected, resulting in a 12.11 % speed reduction [18].

The wave height and period generated by the merchant vessel were calculated using Eq. (4)-(5) [19]

$$H_{W_M} = (\frac{K_W B_M}{L_M})\frac{V_M^2}{g} \tag{4}$$

$$T_{W_M} = \lambda/V_M \cos\theta \tag{5}$$

In Eq. (4)-(5), H_{W_M}, T_{W_M} are the wave height and wave period generated by the merchant vessel,V_M, L_M, B_M are respectively the speed, length, and beam of the vessel. K_w is a coefficient depending on $V/L^{0.5}$, r is the yaw rate from the Nomoto model, and θ is $35^0 16'$for Fr less than 0.7. The 1st order Nomoto model rudder angle and speed to calculate the side force generated by the rudder movement and speed loss due to this force. This alternating force has alternating pressure areas. Calculated the pirate vessels added resistance due to the side force of the merchant vessel [20],

$$F_{SM} = \eta 18.04 A_R V_M^2 \delta \tag{6}$$

$$F_P = \frac{1}{2}\rho C_D A u_{wash}^2 \tag{7}$$

In Eq. (6)-(7), here F_M is the force acting on the merchant vessel's rudder, A_R is the rudder area,V_M speed and δ is the rudder angle. F_{SM} is the side force generated by the rudder, η is the efficiency between 0.7 and 0.8 calculated from [18]. F_p is the drag force acting on the pirate vessel. C_D is drag coefficient, u_{wash} is the propeller wash.

Calculated the pirate vessels added resistance due to wave reflection [21]

$$Rawr, irr = \frac{1}{2}\rho g \zeta_a^2 B_p B_F \alpha_T (1 + a_U)(\frac{0.19}{C_{BP}})(\frac{\lambda}{L_P})^{Fr-1.11} \tag{8}$$

$$R_C = \frac{1}{2}\rho C_f S_P V_P^2 \tag{9}$$

Here in Eq. (8)-(9), $R_{awr,irr}$ is the resistance due to wave height, R_C is the calm-water resistance, B_P is the pirate vessel's beam, B_f is the wave reflection form factor, α_T is the thrust-deduction factor, α_U is the wake-fraction, C_B is the hull's block coefficient, λ is the wavelength, L_P is the pirate vessel length. C_f is the ITTC friction coefficient, S is the wetted surface area, ρ is the seawater density. Calculated the pirate vessels' speed loss due to added resistance under constant brake power,

$$\Delta V = \frac{38H_{W_M}^2}{V_P}(\frac{\lambda}{L_P})^{Fr-1.11} + \frac{F_P}{m}T_{MW} \tag{10}$$

Here in Eq. (10), ΔV is the speed loss due to the wave height and side force generated by the merchant vessel. Fr is the pirate vessel's Froude number, m is the mass of the pirate vessel.

4. Results

Our simulation-based evaluation demonstrates the feasibility of the proposed detection and evasion framework. The successful application of a machine-learning object detection system for piracy situation assessment may help develop a proper evasion system in close-call emergencies. The subsequent section presents the findings.

4.1 Pirate Vessel Detection and Threat Assessment

Pirate-boat classifier Fig. 4 - True-positive rates (TPRs) were highest for fishing-boat (84 %) and life-raft (73 %), moderate for canoe (66 %), skiff (68 %), and speedboat (64 %). For the Pirate-weapon classifier Fig. 5 - Melee weapons achieved strong recall, knife and machete at 89 %, crowbar at 84 %, and firearms at slightly lower (gun 78 %, rifle 78 %).

The *background* class, included in evaluation for completeness, achieved 0 % recall in both classifiers, with all samples misclassified as vessel or weapon categories. This was expected, as the training set focused solely on specific boat and weapon classes without dedicated background samples. In deployment, background scenes would be treated as "no detection," though adding diverse negative samples could help reduce false positives in cluttered environments.

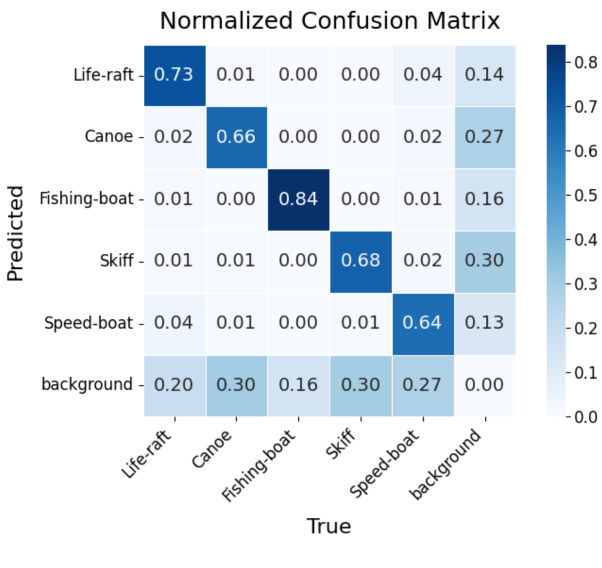

Fig. 4 Pirate-boat confusion matrix (*True(x) vs Predicted(y)*)

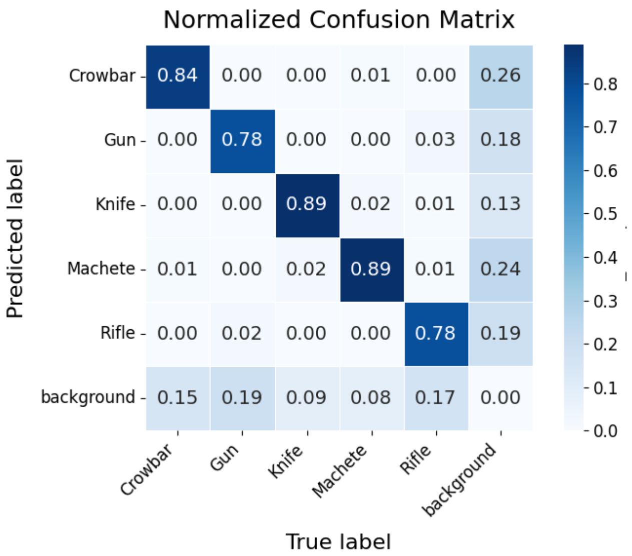

Fig. 5 Pirate-weapon confusion matrix (*True(x) vs Predicted(y)*)

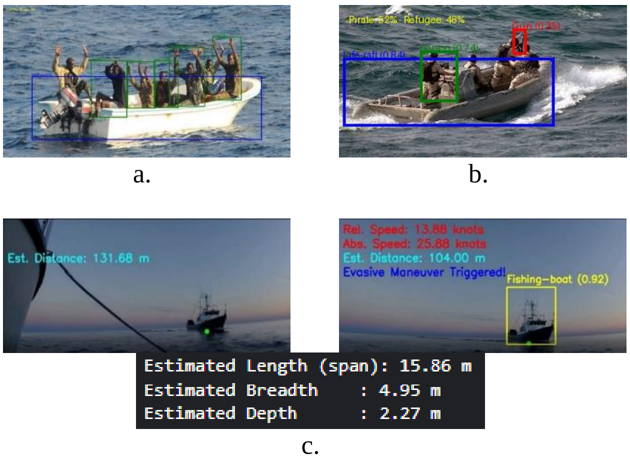

Fig. 6 a. Refugee detection b. Threat detection c. Initial Detection (Frame 1) d. Triggered Evasive Maneuver (Frame 2)

In Fig. 6(a), no weapons are detected, and only people in a life raft are observed, so the vessel is classified as a likely refugee boat with no immediate threat.

In Fig. 6(b), weapons and human presence indicate a moderate threat.

In Fig. 6(c), the vessel identified as a fishing boat (15.86 m × 4.95 m × 2.27 m) poses a moderate risk as it closes in from 131 m to 104 m at a higher speed than the merchant vessel.

4.2 Evasion from Pirate Vessel

For a broader comparison, the speed loss of pirate vessels ranging from 6 m to 20 m, along with that of the fishing vessel, was estimated. Fig. 7 shows that speed loss decreases with increasing vessel length for all rudder angles. Shorter vessels (6–10 m) experience substantial loss, up to 48% at a 10° rudder angle, while vessels near 20 m lose under 5%. In all cases, the zigzag maneuver causes greater speed reduction than a straight course. This also indicates that the maneuvering capabilities of the pirate vessel decrease as the Nomoto time constant. $T = T'L/U$ increase and gain $K = K'U/L$ decreases indicating maneuvering difficulties.

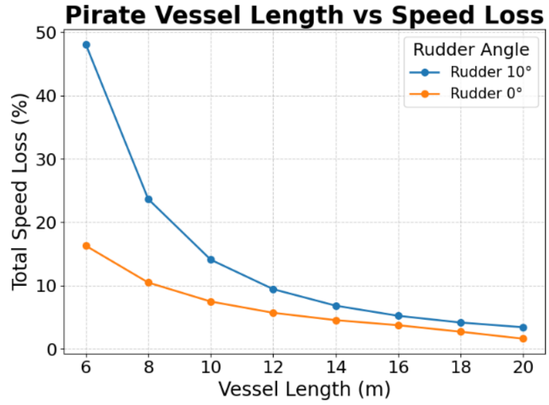

Fig. 7 Pirate vessel speed loss w.r.t vessel size

5. Conclusion

This paper presents a conceptual integrated, machine-learning–driven framework for early piracy detection and an automated evasion decision-making system. By leveraging a YOLOv8 detector trained on a rich maritime piracy dataset augmented for low-light, adverse-weather, and infrared conditions and a probabilistic threat-level assessment incorporating vessel size, speed, and relative direction, our approach reliably discriminates between hostile skiffs and benign craft (e.g., refugee boats).

Using these detection capabilities, an optimal evasive maneuver strategy based on a ±10° zigzag pattern was developed. Simulations show that this maneuver significantly reduces the speed and handling of pursuing pirate vessels, increasing the chances of avoiding an attack when unarmed, consistent with findings from large-scale studies. Combining automated detection with decision-making helps the system guide crews clearly and practically during high-risk situations.

This work has two main limitations: a lack of labeled piracy-incident data, which makes it harder for the model to handle unusual cases, and no measurement of how zigzag maneuvers affect nearby vessels yet. Future work will involve adding more data, including challenging and synthetic examples, integrating inputs from onboard sensors such as radar and inertial systems, and testing the system in real ship trials. This low-cost, flexible system provides a strong base for the next generation of autonomous maritime security solutions.

6. References

[1] O. Melnyk, S. Onyshchenko, and K. Koryakin, “NATURE AND ORIGIN OF MAJOR SECURITY CONCERNS AND POTENTIAL THREATS TO THE SHIPPING INDUSTRY,” *SJSUT.ST*, vol. 113, pp. 145–153, Dec. 2021, doi: 10.20858/sjsutst.2021.113.11.

[2] [Z. He, C. Wang, J. Gao, and Y. Xie, “Assessment of global shipping risk caused by maritime piracy,” *Heliyon*, vol. 9, no. 10, p. e20988, Oct. 2023, doi: 10.1016/j.heliyon.2023.e20988.

[3] W. Bryant, M. Townsley, and B. Leclerc, “Preventing maritime pirate attacks: a conjunctive analysis of the effectiveness of ship protection measures recommended by the international maritime

organisation," *J Transp Secur*, vol. 7, no. 1, pp. 69–82, Mar. 2014, doi: 10.1007/s12198-013-0130-2.

[4] A. Hassani, "Somali pirates say hijacked ship MV Abdullah released after $5 million ransom was paid," *Reuters*, 14 April, 2024. Accessed: 22 May, 2025. [Online]. Available: https://www.reuters.com/world/africa/somali-pirates-say-they-hijacked-ship-mv-abdullah-released-after-5-million-2024-04-14/

[5] "Piracy Reports." Accessed: 08 August, 2025. [Online]. Available: https://www.imo.org/en/ourwork/security/pages/piracy-reports-default.aspx

[6] T. Greminger and N. Al-Rodhan, "Maritime Security: Piracy in the Gulf of Guinea," *Maritime Security*, no. 1.

[7] T. C. Nwokedi, J. Anyanwu, M. Eko-Rapheaels, C. Obasi, I. D. Akpufu, and D. B. Ogola, "Probability Theory Analysis of Maritime Piracy and the Implications for Maritime Security Governance," *JEMS*, vol. 10, no. 2, pp. 133–143, Jun. 2022, doi: 10.4274/jems.2022.37132.

[8] M. Q. Mejia, C. Kojima, and M. Sawyer, Eds., *Piracy at Sea*, vol. 2. in WMU Studies in Maritime Affairs, vol. 2. Berlin, Heidelberg: Springer Berlin Heidelberg, 2013. doi: 10.1007/978-3-642-39620-5.

[9] I. Okafor-Yarwood, O. Eastwood, N. Chikowore, and L. De Oliveira Paes, "Technology and maritime security in Africa: Opportunities and challenges in the Gulf of Guinea," *Marine Policy*, vol. 160, p. 105976, Feb. 2024, doi: 10.1016/j.marpol.2023.105976.

[10] Z. Yang *et al.*, "UAV remote sensing applications in marine monitoring: Knowledge visualization and review," *Science of The Total Environment*, vol. 838, p. 155939, Sep. 2022, doi: 10.1016/j.scitotenv.2022.155939.

[11] J. M. Shane, E. L. Piza, and M. Mandala, "Situational crime prevention and worldwide piracy: a cross-continent analysis," *Crime Sci*, vol. 4, no. 1, p. 21, Dec. 2015, doi: 10.1186/s40163-015-0032-7.

[12] Md. Sabbir Ahmed, "Custom piracy vessel detection dataset." [Online]. Available: Access available upon reasonable request to the authors.

[13] S. Carrillo and J. Contreras, "Obtaining First and Second Order Nomoto Models of a Fluvial Support Patrol using Identification Techniques," *cienc. tecnol. buques*, vol. 11, no. 22, p. 19, Mar. 2018, doi: 10.25043/19098642.160.

[14] K. Zelazny, "Approximate Method of Calculating Forces on Rudder During Ship Sailing on a Shipping Route," *TransNav*, vol. 8, no. 3, pp. 459–464, 2014, doi: 10.12716/1001.08.03.18.

[15] T. I. Fossen, "HANDBOOK OF MARINE CRAFT HYDRODYNAMICS AND MOTION CONTROL".

[16] "ClassNK Register of Ships - M/S ABDULLAH(CNo.151242)." Accessed: 27 June, 2025. [Online]. Available: https://www.classnk.or.jp/register/regships/one_dsp.aspx?imo=9745598&utm_source

[17] K. Al-Salem, W. Al-Nassar, and A. Tayfun, "Risk analysis for capsizing of small vessels," *Ocean Engineering*, vol. 33, no. 5–6, pp. 788–797, Apr. 2006, doi: 10.1016/j.oceaneng.2005.07.003.

[18] Z. Chuang and S. Steen, "Speed loss due to seakeeping and maneuvering in zigzag motion," *Ocean Engineering*, vol. 48, pp. 38–46, Jul. 2012, doi: 10.1016/j.oceaneng.2012.04.009.

[19] R. M. Sorensen, "Prediction of Vessel-Generated Waves with Reference to Vessels Common to the Upper Mississippi River System."

[20] K. J. Rawson and E. C. Tupper, Eds., *Basic ship theory*, 5th ed. [combined volume]. Boston: Butterworth-Heinemann, 2001.

[21] X. Lang and W. Mao, "A Practical Speed Loss Prediction Model at Arbitrary Wave Heading for Ship Voyage Optimization," *J. Marine. Sci. Appl.*, vol. 20, no. 3, pp. 410–425, Sep. 2021, doi: 10.1007/s11804-021-00224-z.